

## Universal Impedance Fluctuations in Wave Chaotic Systems

Sameer Hemmady,<sup>\*</sup> Xing Zheng,<sup>†</sup> Edward Ott,<sup>\*,†</sup> Thomas M. Antonsen,<sup>\*,†</sup> and Steven M. Anlage<sup>\*,‡</sup>

*Physics Department, University of Maryland, College Park, Maryland 20742-4111, USA*

(Received 26 December 2003; revised manuscript received 7 May 2004; published 6 January 2005)

We experimentally investigate theoretical predictions of universal impedance fluctuations in wave chaotic systems using a microwave analog of a quantum chaotic infinite square well potential. We emphasize the use of the *radiation impedance* to remove the nonuniversal effects of the particular coupling between the outside world and the scatterer. Specific predictions that we test include the probability density functions (PDFs) of the real and imaginary parts of the universal impedance, the equality of the variances of these PDFs, and the dependence of these PDFs on a single loss parameter.

DOI: 10.1103/PhysRevLett.94.014102

PACS numbers: 05.45.Mt, 05.45.Gg, 41.20.Jb, 84.40.Az

There is interest in the small wavelength behavior of quantum (wave) systems whose classical (ray orbit) limit is chaotic. Despite their apparent complexity, quantum chaotic systems have remarkable universal properties. Much prior work has focused on identifying the universal statistical properties of wave chaotic systems such as quantum dots and atomic nuclei [1–3]. For example, the nearest neighbor energy level spacing statistics of these systems have universal distributions that fall into one of three classes, depending on the existence or absence of time-reversal symmetry and symplectic properties. Likewise, the eigenfunctions of wave chaotic systems have universal statistical properties, such as one-point and two-point statistical distribution functions [4–6]. It has been challenging to experimentally measure the corresponding universal properties of the scattering and impedance matrices of lossy multiport wave chaotic systems. Here, we experimentally examine universal statistical properties of the complex impedance (or scattering) fluctuations of such systems.

We consider wave systems in the semiclassical limit consisting of enclosures that show chaos in the ray limit, but which are also coupled to their surroundings through a finite number of leads or ports, and also include loss. Examples include quantum dots together with their leads, wave chaotic microwave or acoustical cavities together with their coupling ports, or scattering experiments on nuclei or atoms. Theoretical studies of chaotic scattering have examined the eigenphases of the scattering ( $S$ ) matrix [7], the time-delay distribution [8–10], and the distribution of the scalar reflection and transmission coefficients [10–13]. Experimental work has concentrated on the energy decay and  $S$ -matrix autocorrelation functions in chaotic systems [14–17], and most recently the distribution of scalar reflection coefficients [18]. In the related field of statistical electromagnetism [19], the statistical distribution of electromagnetic fields [20] and impedance [21] within complicated enclosed systems has been studied, but these results have not been generalized to other wave chaotic systems.

Reference [18] (and references therein) takes into account both coupling and absorption in order to apply predictions of random matrix theory (RMT) for the scattering matrices of real systems. There, the average of the reflection coefficient was measured in chaotic microwave cavities, and excellent agreement was found with the predictions of RMT. To remove the nonuniversal effect of the coupling configuration, Ref. [18], as advocated in previous theoretical approaches [22], uses the reflection coefficient averaged over a frequency range  $\Delta f$  that is small compared to  $f$  but large compared to the mean mode frequency spacing. Thus the data for the chaotic cavity with losses is used to extract the universal properties from the same data. Since these nonuniversal properties are due to the detailed coupling geometry, it would seem useful to experimentally extract the characterization of the nonuniversal coupling from a measurement that depends only on the coupling geometry and not on the cavity geometry and losses. In addition, rather than by use of averaging (which results in  $\Delta f$  dependent statistical error), it would also seem desirable to obtain this characterization from a single deterministic measurement at one frequency. This is achieved here for the first time through measurement of the radiation impedance of the ports.

Our purpose is to test specific predictions of RMT using an experiment that allows contact to both the quantum chaotic and wave chaotic aspects of the problem. We use a quasi-two-dimensional chaotic microwave resonator [23] (see insets in Fig. 1) to experimentally study the impedance (which will be defined subsequently) and scattering properties of wave chaotic cavities, including the coupling ports. Through the Helmholtz-Schrödinger analogy for two-dimensional electromagnetic cavities, our results also apply to quantum chaotic systems such as quantum dots.

The theoretical predictions for the impedance matrix are universal and apply to all wave chaotic systems. For example, the real part of the impedance matrix of a wave chaotic system is directly related to the local density of states of mesoscopic metal particles [24]. The NMR line

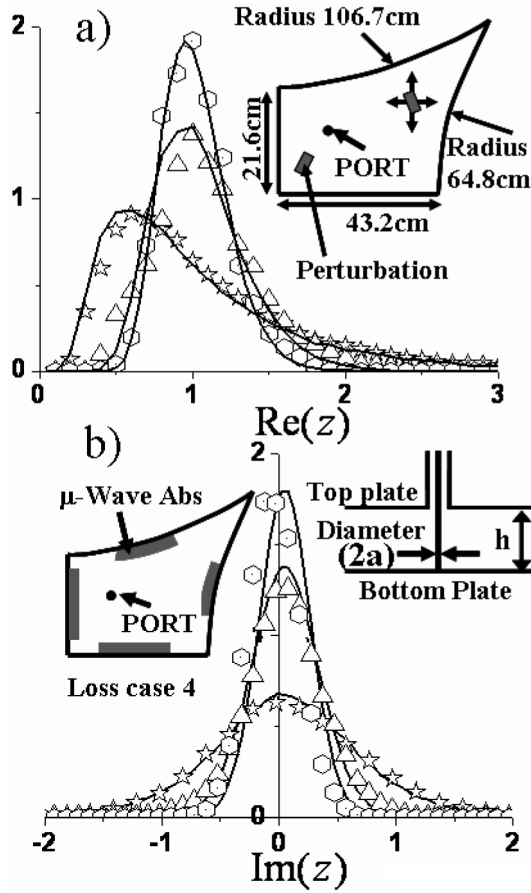


FIG. 1. PDFs for the (a) real and (b) imaginary parts of the normalized cavity impedance  $z$  for a wave chaotic microwave cavity between 7.2 and 8.4 GHz with  $h = 7.87$  mm and  $2a = 1.27$  mm, for three values of loss in the cavity (open stars: zero, triangles: two, hexagons: four strips of absorber). Also shown are single-parameter simultaneous fits for both PDFs. The inset in (a) shows the cavity and the position of the single coupling port. The inset on the left in (b) shows the realization of a high loss cavity (four strips of absorber), while the inset on the right shows the details of the antenna in cross section.

shape of nm-scale metal clusters is predicted to be given by the probability density function (PDF) of  $\text{Re}[z]$  given below [24,25], and is in good agreement with experiment [26]. Wigner introduced a related quantity, the  $R$  matrix, as an alternative method to describe scattering problems [27] in quantum mechanics. In this case, space is divided into two parts: a finite interior domain containing the scattering potential of interest, and the remaining external asymptotic region. The  $R$  matrix describes the boundary condition linearly relating the normal ( $n$ ) derivative of the wave function ( $\hat{\psi}$ ) to the wave function itself at the boundary of the interior domain as  $\hat{\psi} = \vec{R}\partial\hat{\psi}/\partial n$ . The analogous quantity in an electromagnetic system is the impedance matrix  $\vec{Z}$ , relating voltages ( $\hat{V}$ ) and currents ( $\hat{I} \sim \partial\hat{V}/\partial n$ ) at the ports as  $\hat{V} = \vec{Z}\hat{I}$ . The impedance matrix is related to the scattering matrix through  $\vec{S} = \vec{Z}_0^{1/2}(\vec{Z} + \vec{Z}_0)^{-1} \times (\vec{Z} - \vec{Z}_0)\vec{Z}_0^{-1/2}$ , where  $\vec{Z}_0$  is a diagonal real matrix whose

elements are the characteristic impedances of the transmission line modes connected to each port. In what follows, we treat the case where only one port is connected to the cavity so that  $\vec{Z}_0$ ,  $\vec{Z}$ , and  $\vec{S}$  are replaced by scalars,  $Z = Z_0(1 + S)/(1 - S)$ .

In [28] a model is proposed which describes the elements of the  $Z$  matrix for the chaotic cavity. The elements are statistical quantities and are constructed using RMT in conjunction with the following system-specific information: the radiation impedances of the ports, the average spacing of modes of the cavity, and the degree of distributed loss in the cavity. The radiation impedance  $Z_{\text{rad}}$  is the complex impedance seen at the input of the coupling structure for the same coupling geometry but with the side walls of the cavity removed to infinity so that no launched waves return to the port. The real part of the radiation impedance contains information about the waves carried away from the port while the imaginary part contains information about the fields near the port. The radiation impedance is a frequency dependent, system-specific quantity and can be measured directly as will be described. The case of “perfect coupling” requires two conditions:  $\text{Im}\{Z_{\text{rad}}\} = 0$  and  $\text{Re}\{Z_{\text{rad}}\} = Z_0$  and thus almost never occurs in practice. On the other hand, universal results for the statistics of the impedance and scattering characteristics are most commonly formulated for this perfect coupling case.

Reference [28] shows that the normalized impedance  $z = (Z_{\text{cav}} - i\text{Im}[Z_{\text{rad}}])/\text{Re}[Z_{\text{rad}}]$  will be a universal quantity even when data is collected over a range of frequencies for which the value of  $Z_{\text{rad}}$ , and consequently the coupling, varies. In the case of a cavity with no internal losses, the imaginary part of  $z$  is expected to exhibit a Lorentzian probability distribution with unit width [28,29]. Losses manifest themselves through a nonzero real part of  $z$  and lead to the truncation of the tails of the lossless (Lorentzian) distribution of  $\text{Im}[z]$ . It is also predicted that when losses are distributed, the variances of the  $\text{Re}[z]$  and  $\text{Im}[z]$  PDFs are equal and given by  $\sigma_{\text{Re}z}^2 = \sigma_{\text{Im}z}^2 = Q/(\pi\tilde{k}^2)$  in the case of time-reversal symmetric wave chaotic systems (Gaussian orthogonal ensemble) [28]. Here  $\tilde{k}^2 = k^2/\Delta k^2$ , where  $k$  is the free space wave number,  $\Delta k^2$  is the mean spacing in  $k^2$  eigenvalues for the closed cavity ( $\Delta k^2 = 4\pi/A$  for a two-dimensional cavity of area  $A$ ), and  $Q$  is the quality factor of the enclosure due to internal losses. The parameter  $\tilde{k}^2/Q$  represents the ratio of the resonance width to the mean level spacing, similar to that defined in other RMT treatments [13,25]. The theory also makes quantitative predictions for the PDFs of  $\text{Re}[z]$  and  $\text{Im}[z]$  dependent only on this parameter.

We note that characterizing the losses in terms of a single-parameter  $Q$  is an approximation. If there are losses due to spatially localized coupling of energy out of the cavity they should be treated as additional ports with their own radiation resistances. However, if the number of such ports is large [16,18] and they are well separated physi-

cally, then the losses can be treated as being distributed and characterized by a single parameter.

For our experimental tests of the theory, the single driving port consists of the center conductor of a coaxial cable that extends from the top lid of the cavity and makes contact (shorts) with the bottom plate [Fig. 1(b) right inset], injecting current into the bottom plate of the cavity. This gives rise to a normalized resonance width due to coupling  $\tilde{k}^2/Q_{\text{coup}} \approx 0.03\text{--}0.12$  in this experiment between 7.2 and 8.4 GHz, depending on antenna and cavity geometry. To perform ensemble averaging, two perturbations [gray rectangles in Fig. 1(a) inset], made up of rectangular ferromagnetic solids wrapped in Al foil (dimensions  $26.7 \times 40.6 \times 7.87 \text{ mm}^3$ ), are systematically scanned and rotated throughout the volume of the cavity by means of a strong magnet that is placed outside the cavity.

As predicted, the universal cavity impedance statistics can be drawn from  $S$  measurements of the cavity (referred to as the cavity case) and a measurement with identical coupling, but with the walls of the cavity removed to infinity (the radiation case). The latter condition is realized experimentally by placing microwave absorber (ARC tech-DD10017D,  $< -25 \text{ dB}$  return loss between 6 and 12 GHz) along all the sidewalls of the cavity. An ensemble of wave chaotic cavities is obtained by recording  $S$  as a function of frequency (8001 points between 6 and 12 GHz) for 100 different positions and orientations of the perturbations within the cavity.

Figure 1 shows the evolution of the PDFs for the normalized cavity impedance in the presence of increasing loss. The losses are incrementally increased within the cavity by placing 15.2 cm-long strips of microwave absorber along the inner walls of the cavity. The inset in Fig. 2 shows the reflection spectra  $|S|$  for the radiation case as well as loss case 0 (which corresponds to the empty cavity with no microwave absorber strips) and loss case 4 (Fig. 1 left inset). The data in Fig. 1 show that as the losses within the cavity increase, the PDF of the normalized imaginary part of the impedance loses its long tails and begins to sharpen up, developing a Gaussian appearance. The normalized PDF of the real part smoothly evolves from being peaked below 1 into a Gaussian-like distribution that peaks at 1 and sharpens with increasing loss. The PDF data is overlaid with a single-parameter fit to the theory, which simultaneously fits both the real and imaginary histograms for each loss scenario. There is a close overlap between the theoretical prediction and the experimental results with a choice of  $\tilde{k}^2/Q = 0.8, 4.2,$  and  $7.6$  in order of increasing loss (i.e., imaginary part of the resonant frequency). This is in good agreement with the typical  $Q$  values for the cavity (e.g., about 200 at  $\tilde{k}^2/Q = 0.8$ ) extracted from  $S_{11}(\omega)$  measurements for these different loss scenarios.

In Fig. 2 we test another prediction of our theory which concerns the variance of the PDFs and its relation to the

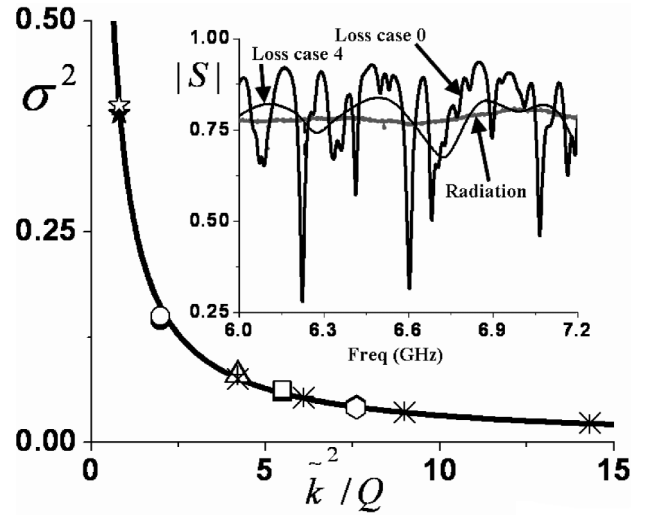


FIG. 2. Plot of PDF variances for  $\text{Re}[z]$  (open) and  $\text{Im}[z]$  (closed) for  $h = 7.87 \text{ mm}$  and  $7.2\text{--}8.4 \text{ GHz}$  versus fit parameter  $\tilde{k}^2/Q$  that simultaneously fits both PDFs. Also shown are similar data for the case  $h = 1.78 \text{ mm}$  for  $\text{Re}[z]$  (+) and  $\text{Im}[z]$  ( $\times$ ) for the  $6\text{--}7.2, 7.2\text{--}8.4, 9\text{--}9.75,$  and  $11.25\text{--}12 \text{ GHz}$  ranges. The solid line is the best fit to all the data points. Inset shows the reflection spectra  $|S|$  from 6 to 7.2 GHz for two loss cases (loss case 0: no absorber and loss case 4: four strips of absorber), and the radiation case.

control parameter  $\tilde{k}^2/Q$ . We can systematically change the  $Q$  by changing the cavity height ( $h$ ) and the amount of microwave absorber along the interior walls, and we change  $\tilde{k}^2$  by changing the frequency. Figure 2 shows the variance of the experimental PDFs of the real and imaginary parts of  $z$  compared to the  $\tilde{k}^2/Q$  fit parameter for the same PDFs for a number of cases. The open symbols (+ symbols) are the variance of the real part of  $z$  for a cavity height of  $h = 7.87 \text{ mm}$  ( $h = 1.78 \text{ mm}$ ); the closed symbols ( $\times$  symbols) are the variance of the imaginary part of  $z$  for  $h = 7.87 \text{ mm}$  ( $h = 1.78 \text{ mm}$ ). The best-fit hyperbola (solid line in Fig. 2) has a coefficient of  $0.32 \pm 0.01$ , while the theory [28] predicts it to be  $1/\pi \approx 0.32$ . We also note a close overlap between the variances of  $\text{Re}[z]$  and  $\text{Im}[z]$  consistent with the prediction that they are equal in the limit  $Q \gg 1$  [28].

We also test the degree of insensitivity of the universal properties of the normalized impedance PDFs to details and nonuniversal quantities. Working in the 9 to 9.6 GHz range, we take two identical cavities and change only the diameter of the coupling wire in the antenna from  $2a = 1.27 \text{ mm}$  to  $0.635 \text{ mm}$ . As seen in Fig. 3(a), this difference causes a dramatic change in the raw  $\text{Im}[Z_{\text{cav}}]$  PDF. However, in agreement with the theoretical prediction, this difference essentially disappears in the PDFs for the appropriately scaled impedance  $z$  as shown in Fig. 3(b).

The results tested here are based on very general considerations and should apply equally well to conductance measurements through quantum dots, impedance, or scat-

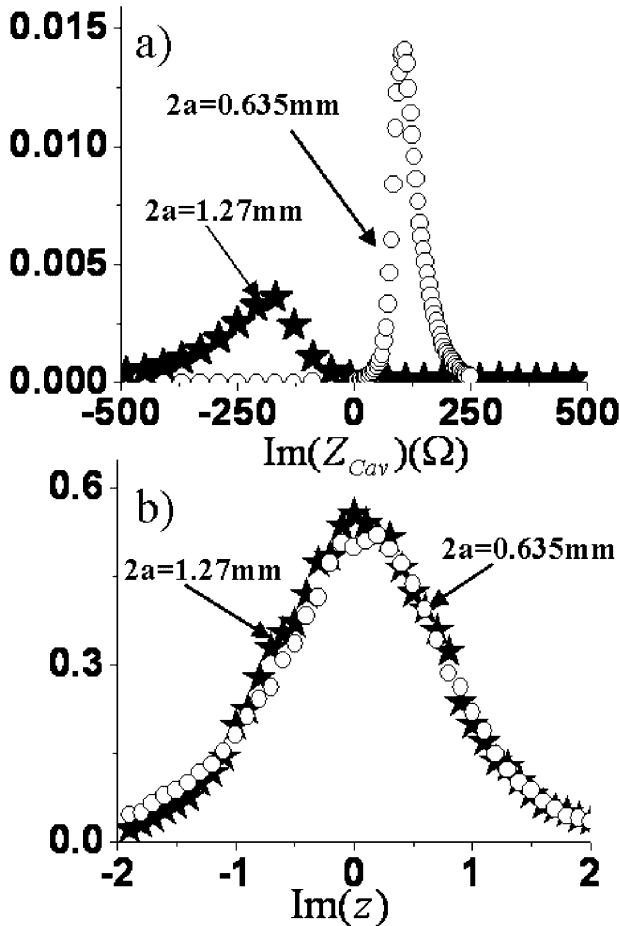


FIG. 3. (a) Shows the PDFs of the imaginary part of cavity impedance for two different antenna diameters,  $2a = 0.635 \text{ mm}$  (circles) and  $2a = 1.27 \text{ mm}$  (stars), from 9 to 9.6 GHz. (b) The two curves in (a) scale together using the prescription of theory for the imaginary normalized cavity impedance.

tering matrix measurements on electromagnetic or acoustic enclosures, and scattering experiments from nuclei and Rydberg atoms. In conclusion, we have examined key testable predictions for the statistics of impedance fluctuations and found satisfactory agreement on all experimental issues directly related to the theory. We find that a single-parameter simultaneous fit to two independent PDFs is remarkably robust and successful, and the fit parameter is physically reasonable. The normalized cavity impedance describes universal properties of the impedance fluctuations that depend only on a single control parameter characterizing the cavity loss.

We acknowledge useful discussions with R. Prange and S. Fishman as well as comments from Y. Fyodorov and P. Brouwer. This work was supported by the DOD MURI for the study of microwave effects under AFOSR Grant No. F496200110374.

\*Also with the Department of Electrical and Computer Engineering.

†Also with the Institute for Research in Electronics and Applied Physics.

‡Also with the Center for Superconductivity Research.

- [1] R. U. Haq, A. Pandey, and O. Bohigas, *Phys. Rev. Lett.* **48**, 1086 (1982).
- [2] See H.-J. Stöckmann, *Quantum Chaos* (Cambridge University Press, Cambridge, England, 1999) and references therein.
- [3] Y. Alhassid, *Rev. Mod. Phys.* **72**, 895 (2000).
- [4] C. E. Porter and R. G. Thomas, *Phys. Rev.* **104**, 483 (1956).
- [5] H. Alt *et al.*, *Phys. Rev. Lett.* **74**, 62 (1995).
- [6] V. N. Prigodin *et al.*, *Phys. Rev. Lett.* **75**, 2392 (1995).
- [7] R. Blümel and U. Smilansky, *Phys. Rev. Lett.* **64**, 241 (1990).
- [8] Y. V. Fyodorov and H.-J. Sommers, *J. Math. Phys. (N.Y.)* **38**, 1918 (1997).
- [9] P. Šeba, K. Zyczkowski, and J. Zakrzewski, *Phys. Rev. E* **54**, 2438 (1996).
- [10] D. V. Savin and H.-J. Sommers, *Phys. Rev. E* **68**, 036211 (2003).
- [11] E. Kogan, P. A. Mello, and H. Liqun, *Phys. Rev. E* **61**, R17 (2000).
- [12] C. W. J. Beenakker and P. W. Brouwer, *Physica E (Amsterdam)* **9**, 463 (2001).
- [13] Y. V. Fyodorov, *JETP Lett.* **78**, 250 (2003).
- [14] H. Alt *et al.*, *Phys. Rev. Lett.* **74**, 62 (1995).
- [15] O. I. Lobkis, I. S. Rozhkov, and R. L. Weaver, *Phys. Rev. Lett.* **91**, 194101 (2003).
- [16] R. Schäfer *et al.*, *J. Phys. A* **36**, 3289 (2003).
- [17] J. Barthélemy, O. Legrand, and F. Mortessagne, *cond-mat/0401638*.
- [18] R. A. Méndez-Sánchez *et al.*, *Phys. Rev. Lett.* **91**, 174102 (2003).
- [19] R. Holland and R. St. John, *Statistical Electromagnetics* (Taylor and Francis, Philadelphia, 1999).
- [20] D. A. Hill *et al.*, *IEEE Transactions on Electromagnetic Compatibility* **36**, 169 (1994).
- [21] L. K. Warne *et al.*, *IEEE Trans. Antennas Propag.* **51**, 978 (2003).
- [22] P. A. Mello, P. Pereyra, and T. H. Seligman, *Ann. Phys. (N.Y.)* **161**, 254 (1985).
- [23] A. Gokirmak *et al.*, *Rev. Sci. Instrum.* **69**, 3410 (1998).
- [24] A. D. Mirlin and Y. V. Fyodorov, *Europhys. Lett.* **25**, 669 (1994); A. D. Mirlin, *Phys. Rep.* **326**, 259 (2000).
- [25] K. B. Efetov and V. N. Prigodin, *Phys. Rev. Lett.* **70**, 1315 (1993).
- [26] F. C. Fritschij *et al.*, *Phys. Rev. Lett.* **82**, 2167 (1999).
- [27] E. P. Wigner and L. Eisenburd, *Phys. Rev.* **72**, 29 (1947); A. M. Lane and R. G. Thomas, *Rev. Mod. Phys.* **30**, 257 (1958).
- [28] X. Zheng, T. M. Antonsen, and E. Ott, *cond-mat-0408327* [*J. Electromag.* (to be published)].
- [29] T. J. Krieger, *Ann. Phys. (N.Y.)* **42**, 375 (1967); P. Mello, in *Mesoscopic Quantum Physics*, edited by E. Akkermans *et al.* (Elsevier, Amsterdam, 1995).